Molecular Signature of ^{18}F-FDG PET Biomarkers in Newly Diagnosed Multiple Myeloma Patients: A Genome-Wide Transcriptome Analysis from the CASSIOPET Study

Jean-Baptiste Alberge[1,2], Françoise Kraeber-Bodéré[1–5], Bastien Jamet[2,3], Cyrille Touzeau[1,2,5], Hélène Caillon[5], Soraya Wuilleme[5], Marie-Christine Béné[5], Tobias Kampfenkel[6], Pieter Sonneveld[7], Mark van Duin[7], Herve Avet-Loiseau[8], Jill Corre[8], Florence Magrangeas[1,2,5], Thomas Carlier[1–3], Caroline Bodet-Milin[1–3], Michel Chérel[1,2,4], Philippe Moreau[1,2,5], Stéphane Minvielle[1,2,5], and Clément Bailly[1–3]

[1]*Université de Nantes, CHU Nantes, CNRS, Inserm, CRCINA, Nantes, France;* [2]*Site de Recherche Intégrée sur le Cancer (SIRIC), Imaging and Longitudinal Investigations to Ameliorate Decision-Making (ILIAD), INCA-DGOS-Inserm 12558, Nantes, France;* [3]*Nuclear Medicine Unit, University Hospital, Nantes, France;* [4]*Nuclear Medicine Unit, ICO-Gauducheau, Nantes-Saint-Herblain, France;* [5]*Haematology Department, University Hospital, Nantes, France;* [6]*Janssen Research & Development, LLC, Leiden, The Netherlands;* [7]*Erasmus University Medical Center Cancer Institute, Rotterdam, The Netherlands; and* [8]*Unité de Génomique du Myélome, Institut Universitaire du Cancer de Toulouse, Institut National de la Santé, Oncopole, Toulouse, France*

The International Myeloma Working Group recently fully incorporated ^{18}F-FDG PET into multiple myeloma (MM) diagnosis and response evaluation. Moreover, a few studies demonstrated the prognostic value of several biomarkers extracted from this imaging at baseline. Before these ^{18}F-FDG PET biomarkers could be fully endorsed as risk classifiers by the hematologist community, further characterization of underlying molecular aspects was necessary. **Methods:** Reported prognostic biomarkers (^{18}F-FDG avidity, SUV_{max}, number of focal lesions, presence of paramedullary disease [PMD] or extramedullary disease) were extracted from ^{18}F-FDG PET imaging at baseline in a group of 139 patients from CASSIOPET, a companion study of the CASSIOPEIA cohort (ClinicalTrials.gov identifier NCT02541383). Transcriptomic analyses using RNA sequencing were realized on sorted bone marrow plasma cells from the same patients. An association with a high-risk gene expression signature (IFM15), molecular classification, progression-free survival, a stringent clinical response, and minimal residual disease negativity were explored. **Results:** ^{18}F-FDG PET results were positive in 79.4% of patients; 14% and 11% of them had PMD and extramedullary disease, respectively. Negative ^{18}F-FDG PET results were associated with lower levels of expression of hexokinase 2 (*HK2*) (fold change, 2.1; adjusted $P = 0.04$) and showed enrichment for a subgroup of patients with a low level of bone disease. Positive ^{18}F-FDG PET results displayed 2 distinct signatures: either high levels of expression of proliferation genes or high levels of expression of *GLUT5* and lymphocyte antigens. PMD and IFM15 were independently associated with a lower level of progression-free survival, and the presence of both biomarkers defined a group of "double-positive" patients at very high risk of progression. PMD and IFM15 were related neither to minimal residual disease assessment nor to a stringent clinical response. **Conclusion:** Our study confirmed and extended the association between imaging biomarkers and transcriptomic programs in MM. The combined prognostic value of PMD and a high-risk IFM15 signature may help define MM patients with a very high risk of progression.

Key Words: multiple myeloma, ^{18}F-FDG PET, CASSIOPET study, genome-wide transcriptome, RNA sequencing

J Nucl Med 2022; 63:1008–1013
DOI: 10.2967/jnumed.121.262884

In the past decade, there has been increasing use of PET with ^{18}F-FDG for the staging and therapeutic evaluation of multiple myeloma (MM) patients (*1*). A few studies have demonstrated the prognostic value of several biomarkers extracted from ^{18}F-FDG PET at baseline—the number of focal lesions (FLs), the presence or absence of extramedullary disease (EMD) or paramedullary disease (PMD), and glucose SUV_{max}—as reviewed by Michaud-Robert et al. (*2*). Furthermore, ^{18}F-FDG PET results are considered to be negative in approximately 10%–20% of MM patients (*2*). This pattern, associated with low levels of expression of hexokinase 2 (*HK2*)—an enzyme involved in the first step of glycolysis—is usually described as a false-negative result for disease detection but seems to carry a prognostic value (*3–5*). Before these ^{18}F-FDG PET biomarkers could be fully endorsed as risk classifiers by the hematologist community, further characterization of underlying molecular aspects was necessary. Genome-wide transcriptomic analyses through RNA sequencing characterized, without bias, the gene expression program of tumor cells purified from bone marrow aspirates. RNA sequencing helped researchers to understand the molecular basis of MM complexity (*6,7*) and to identify MM patients who have with gene signatures such as GEP70, EMC-92, or IFM15 and who are at high risk of progression (*8,9*).

The purpose of this study was to identify gene expression patterns associated with prognostic ^{18}F-FDG PET biomarkers in newly diagnosed MM patients included in the prospective multicenter CASSIOPET study. An association with a high-risk gene expression signature, molecular classification, progression-free survival (PFS), a clinical response, and minimal residual disease (MRD) negativity at 100 d after autologous stem cell transplant (ASCT) were also explored.

Received Jul. 9, 2021; revision accepted Oct. 14, 2021.
For correspondence or reprints, contact Clément Bailly (clement.bailly@chu-nantes.fr) or Stéphane Minvielle (stephane.minvielle@univ-nantes.fr).
Published online Jan. 27, 2022.

MATERIALS AND METHODS

Patients

A group of 139 newly diagnosed patients from CASSIOPET (*5*) (Françoise Kraeber-Bodéré et al., unpublished data, 2020), a companion study of the phase 3 CASSIOPEIA trial (*10*), underwent gene expression profiling at baseline in addition to ^{18}F-FDG PET imaging. The aims and inclusion and exclusion criteria of the CASSIOPEIA trial (ClinicalTrials.gov identifier NCT02541383) were previously reported (*10*). The CASSIOPET study was locally approved by the institutional ethics committee (University Hospital, Nantes, France). Myeloma plasma cells were derived from bone marrow samples collected at the Intergroupe Francophone du Myélome and the Dutch/Belgian Haemato-Oncology Foundation for Adults in The Netherlands. Myeloma cells were purified using nanobeads and an anti-CD138 antibody (RoboSep; Stem Cell Technologies). The average MM cell purity was greater than 99% (range, 79%–100%), as assessed by May-Grunwald Giemsa staining and morphology. Finally, all samples with available material containing greater than 200 ng of RNA and an RNA integrity number of greater than 6.5 were included and sequenced.

RNA Sequencing

Libraries were prepared with NEBNext Ultra II for a directional RNA sequencing kit (reference: E7765 L, E7490 L, E6440S; New England Biolabs). Quality controls were performed with High Sensitivity D1000 (Agilent) and an NEBNext Library Quant Kit for Illumina (reference: E7630 L) on a TapeStation 2200 (Agilent). All libraries passed quality controls and were sequenced on a NovaSEquation 6000 (Illumina) with S2 flow cells at 2 × 100 cycles (reference: 20012861). Finally, the sequencing depth ranged from 74 to 163 million paired reads per library. RNA sequencing reads were aligned to the human reference genome hg38/GRCh38.p13, and genes were quantified with STAR v2.7.3 and Ensembl v99 (both products open source data/software). Standardized $\log_2$ values of transcripts per million units were used to compute high-risk and molecular classification scores after the removal of immunoglobulin genes (*11*). The threshold for high-risk classification with IFM15 ($x = 1.3$) was defined according to Decaux et al. (*9*). The maximum of the weighted means was used to classify patients in the 7 subgroups of the University of Arkansas for Medical Sciences (UAMS) classification (*6*) and determine the GEP70 signature. DESeq2 (open source R/Bioconductor package) was used to perform differential expression analysis from raw counts with plasma cell purity and site of collection (Intergroupe Francophone du Myélome or Haemato-Oncology Foundation for Adults in The Netherlands) treated as model covariates. The DESeq2 variance stabilizing transformation was used for graphical representation and statistical analysis of gene expression levels.

^{18}F-FDG PET Evaluation

^{18}F-FDG PET images were acquired at baseline according to the local protocol at each center and the recommendations of good practice for PET imaging. Briefly, all patients fasted for at least 4 h before ^{18}F-FDG injection. The blood glucose level measured before ^{18}F-FDG administration had to be ≤150 mg/dL. Whole-body imaging was performed between 60 and 80 min after ^{18}F-FDG injection (3–7 MBq/kg). ^{18}F-FDG PET data were centrally collected and analyzed, with masking of patient treatment and follow-up, by an independent team of nuclear medicine physicians with extensive experience in MM. As previously described (*2,12*) and used in the CASSIOPET protocol, ^{18}F-FDG PET negativity, number of bone FLs (defined as the presence of areas of focally increased tracer uptake in bone, with or without any underlying lytic lesion on CT, and present on at least 2 consecutive slices), and presence of EMD (defined as tracer uptake in tissue not contiguous to bone) or PMD (defined as soft-tissue invasion with contiguous bone involvement) were reported. The bone SUV_{max} was determined; it was defined as the highest SUV_{max} on bone analysis, including FLs, PMD, and medullary uptake (measured at the lumbar vertebrae [L3–L5] and excluding focal lesions with a 3-dimensional rectangular region of interest).

MRD Assessment and Clinical Response

As reported in the CASSIOPEIA trial, MRD was evaluated by multiparametric flow cytometry of bone marrow aspirates at 100 d after ASCT. MRD negativity was defined as less than 0.001% of aberrant clonal plasma cells (10^{-5} threshold). The clinical response was assessed according to International Myeloma Working Group criteria at 100 d after ASCT (*13*).

Statistical Analysis

Quantitative biologic and clinical variables were described with the median and interquartile range or with the mean and SD. The significance of the average difference between groups was assessed with the Kruskal–Wallis method and the Dunn post hoc approach for multiple-group testing or the Wilcoxon test for 2 groups. Differences in distribution between groups were assessed with a χ^2 Pearson test (or a Fisher exact test, if appropriate). Absolute χ^2 residuals of greater than 2 were considered significant, as post hoc. A DEseq2 Wald test was used to assess differences in gene expression between groups. For survival analysis, PFS was calculated from randomization date to disease progression or death, whichever occurred first, or to the last follow-up date. Hazard ratios (HRs) between groups were calculated with a Cox model. Survival curves were calculated using the Kaplan–Meier method, and groups were compared using a likelihood ratio test. *P* values were corrected for multiple-group testing with the Benjamini–Hochberg method. Adjusted *P* values of less than 0.05 were considered significant. All calculations were performed with R 3.6.0. (R Foundation).

RESULTS

Demography and ^{18}F-FDG PET Results

Of the 268 patients in the CASSIOPET study, 139 patients were considered for this analysis. Because bone marrow aspiration samples for transcriptomic analyses using RNA sequencing were not mandatory in the CASSIOPET trial at diagnosis, 129 patients were enrolled in CASSIOPET before the start of this ancillary work or did not have sufficient materials available for this analysis. The included patients had demographic and clinical characteristics (age, sex, Revised International Staging System [R-ISS] staging, high-risk cytogenetics, treatment arms) similar to those of the entire CASSIOPET population (Supplemental Table 1). Our cohort included 110 patients with positive ^{18}F-FDG PET results (79%), of whom 20 (14%) and 16 (12%) had PMD and EMD, respectively, at baseline. The median baseline SUV_{max} was 3.2 (ranging from 1.5 to 12), with 35 (32%) of the 110 ^{18}F-FDG–avid MM patients having an SUV_{max} higher than 4.2. Sixty-four (46%) of our patients had 3 or more FLs, and 27 (19%) showed diffuse medullary uptake higher than the liver background. The main characteristics of our cohort with regard to ^{18}F-FDG PET imaging and gene signatures are shown in Supplemental Figure 1.

Molecular Profile of Patients with Negative Results on PET Scans

To understand which patients were most likely to have negative or normal ^{18}F-FDG PET, we explored the levels of expression of glucose transporters (GLUTs) 1–5 (GLUT1–GLUT5, respectively) and of hexokinases (HKs) 1–3 (HK1–HK3, respectively). *HK2* was expressed less in patients with normal ^{18}F-FDG PET results (fold change [FC], 2.0; $P = 0.04$) (Fig. 1A) and to a lesser extent than *GLUT5* (*SLC2A5*; FC, 4.2; $P = 7 \times 10^{-4}$), which codes for a canonical fructose receptor (*14*). Conversely, *GLUT3* (*SLC2A3*)

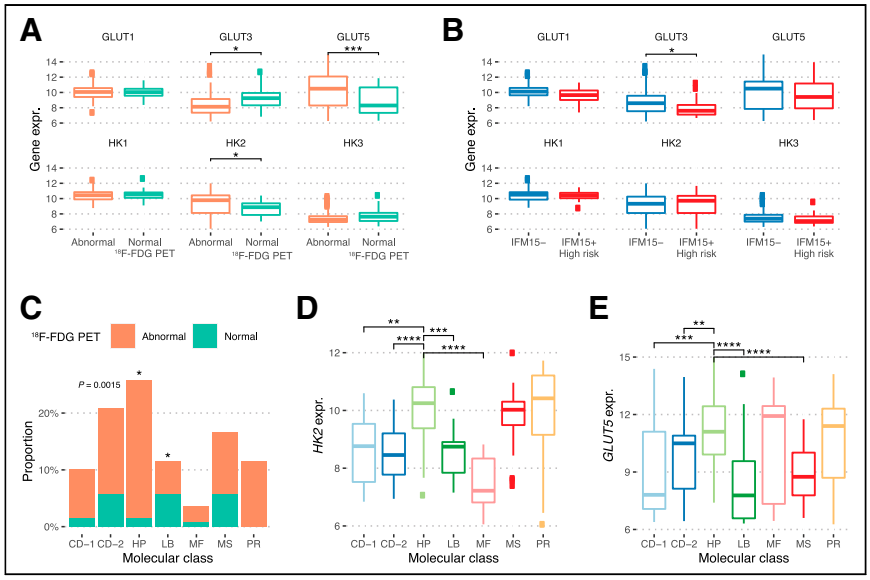

FIGURE 1. Molecular profile of ^{18}F-FDG PET negativity in CASSIOPET trial. (A) Expression (expr.) of GLUTs and HKs on ^{18}F-FDG PET scans with abnormal or positive (orange) vs. normal or negative (green) results in CASSIOPET cohort. (B) Expression of GLUTs and HKs in patients with standard-risk (blue) vs. high-risk (red) IFM15 gene expression signatures. (C) Distribution of normal ^{18}F-FDG PET results across MM molecular classes as defined by UAMS. (D and E) Expression of HK2 (D) and GLUT5 (E) in MM molecular classes. Gene expression levels are given in variance stabilizing transformation–normalized counts (see Materials and Methods). n = 139 patients. $^{*}P < 0.05$. $^{**}P < 0.01$. $^{***}P < 0.001$. $^{****}P < 0.0001$.

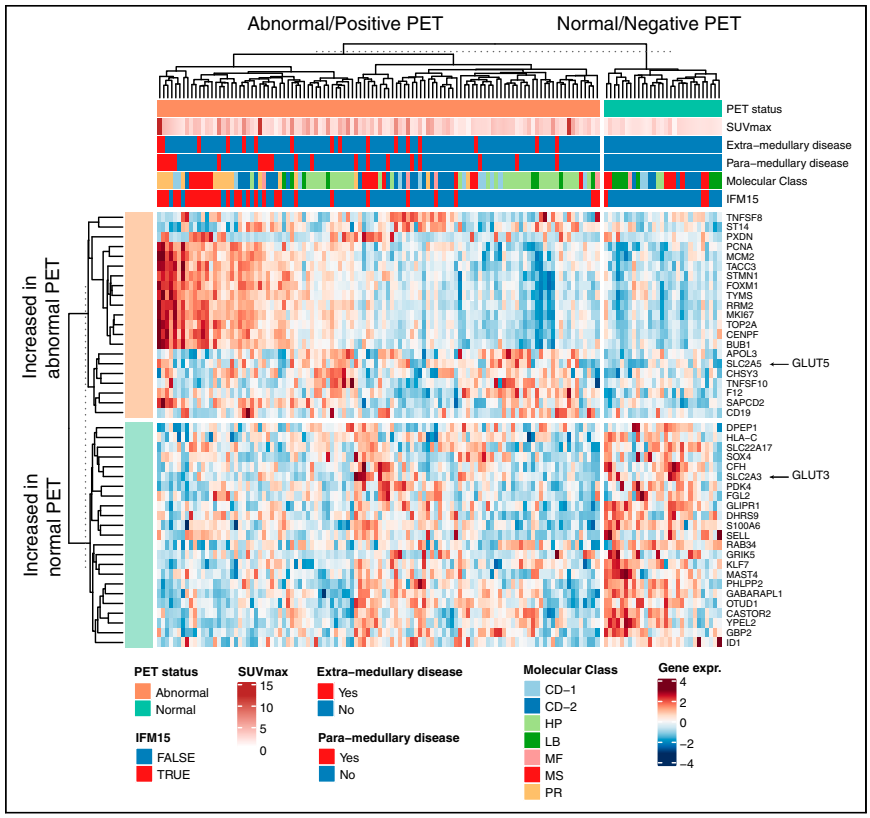

FIGURE 2. Gene expression (expr.) profiling of ^{18}F-FDG PET scans with abnormal results. Heat map representation of standardized gene expression levels of most differentially expressed genes between 2 conditions (normal and abnormal ^{18}F-FDG PET results), obtained with DESeq2. *SLC2A3* encodes GLUT3, and *SLC2A5* encodes GLUT5.

was found to be overexpressed in patients with negative or normal ^{18}F-FDG PET results (FC, 2.0; P = 0.05) (Fig. 1A) as well as in patients assessed with the high-risk IFM15 signature (IFM15+; FC, 2.1; P = 0.01) (Fig. 1B). The expression of other HKs and GLUTs was comparable in both groups (IFM15+ and IFM15−) (Fig. 1B). Of note, *GLUT2* and *GLUT4* were not found to be expressed in this study (0–0.2 transcript per million, on average) and were discarded from the analysis.

The UAMS molecular classification of MM in 7 subgroups (CD-1, CD-2, HP, low level of bone disease [LB], MF, MS, proliferating [PR]) was statistically associated with normal ^{18}F-FDG PET results (Fig. 1C). In particular, an overrepresentation of negative ^{18}F-FDG PET imaging results was found in the LB group of patients compared with the reference group of HP patients. The LB group consistently showed an underexpression of *HK2* ($P = 9 \times 0^{-4}$) and *GLUT5* ($P = 1.6 \times 10^{-5}$) (Figs. 1D and 1E).

Finally, a differential analysis of gene expression performed with DEseq2 for positive or abnormal and negative or normal ^{18}F-FDG-PET results showed that 1,202 genes were deregulated. Genes that were moderately to highly expressed (≥500 messenger RNA [mRNA], on average) and on which the condition had an important effect ($\log_2$ FC, ≥1, in absolute value) are shown in Figure 2. Hierarchical clustering separated 2 groups of patients with positive or normal ^{18}F-FDG PET results and distinct signatures. Ontology analysis confirmed a strong proliferation signature (*MKI-67*, *PCNA*, *TOP2A*, *STMN1*) in a proportion of patients with positive ^{18}F-FDG PET results (Fig. 2; Supplemental Table 2), whereas the other positive scans showed overexpressed lymphocyte antigens (*CD19*, *TNFSF8*/*CD30 L*, *TNFSF10*/*TRAIL*) and *SLC2A5*/*GLUT5*. Conversely, negative or normal ^{18}F-FDG-PET results showed a cellular machinery ontology (secretion, membrane, exocytosis) and regular expression of *SLC2A3*/*GLUT3*, consistent with results presented in Figure 1.

Molecular Profile Associated with ^{18}F-FDG PET Abnormalities

Among patients with positive or abnormal ^{18}F-FDG PET scan results, patients with a high-risk GEP70 signature had more frequent PMD than GEP70-negative patients (P = 0.003) (Supplemental Fig. 2), whereas no association was observed with the IFM15 signature (Fig. 3A). The PR subgroup of

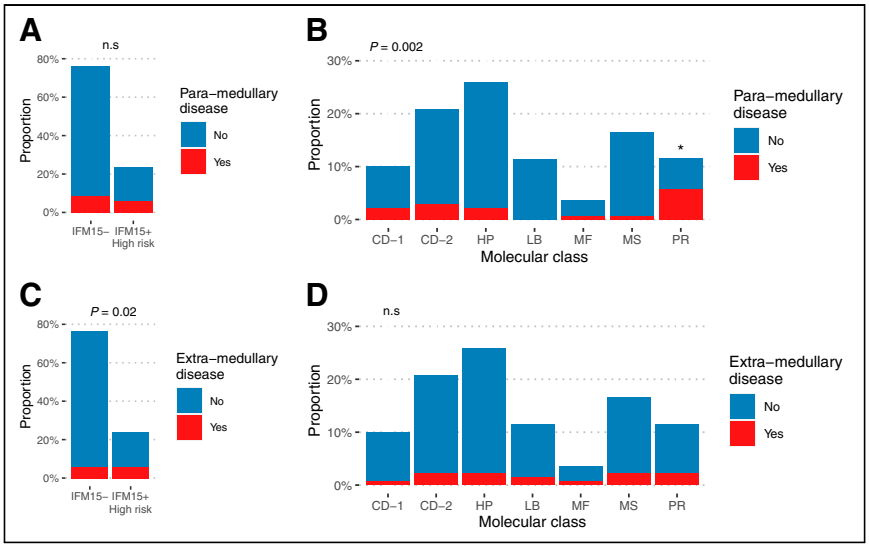

FIGURE 3. Molecular profiles of PMD and EMD on ^{18}F-FDG PET. (A and B) Distribution of patients with PMD at baseline for high-risk and standard-risk IFM15 expression signatures (A) and across myeloma molecular classes (B). (C and D) Distribution of patients with EMD at baseline for high-risk and standard-risk IFM15 expression signatures (C) and across myeloma molecular classes (D). n.s = not significant ($P > 0.05$).

the UAMS molecular classification was associated with PMD ($P = 0.02$), whereas none of the patients in the LB cluster had PMD, despite abnormal ^{18}F-FDG PET scan results (Fig. 3B). Similar analyses for EMD showed a significantly higher proportion in the IFM15+ group ($P = 0.02$) (Fig. 3C) and the lack of a statistical association with GEP70 (Supplemental Fig. 2) or molecular classification (Fig. 3D).

Prognostic Impact of ^{18}F-FDG PET and High-Risk Gene Expression Signatures

The median follow-up time of our cohort was 26 mo (95% CI: 21–33 mo), during which 26 patients (19%) progressed (disease progression or death) and 9 patients (6%) died. Survival analyses were limited to PFS; overall survival was discarded because of the small number of events.

Univariate Cox analysis (Supplemental Tables 3 and 4) showed that imaging biomarkers and gene expression were prognostic for progression. In particular, PMD and IFM15 were strongly associated with relapse (HR for PMD, 5.2 [95% CI, 2.3–11]; HR for IFM15, 4.3 [95% CI, 1.9–9.4]). The combination of PMD and IFM15 in a Cox multivariate model showed the independence of these 2 variables in predicting relapse (HR for PMD, 4.3 [95% CI, 1.9–9.7] [$P < 0.001$]; HR for IFM15, 3.7 [95% CI, 1.6–8.1] [$P = 0.001$]) (Fig. 4A). Of note, both variables remained significant in the model when accounting for R-ISS staging (Supplemental Table 5). Combining both PMD and IFM15 biomarkers defined a group with a very high risk of progression ($P = 4 \times 10^{-5}$) (Fig. 4B). Besides, PMD and IFM15 did not correlate with a deep clinical response, as defined by a complete stringent clinical response or by MRD negativity at 100 d after ASCT (Supplemental Fig. 3).

Similarly, patients with negative or normal ^{18}F-FDG PET results, with a good prognosis, and patients with an IFM15 signature, with a poor prognosis, seemed to complement each other in a Kaplan–Meier analysis and in a Cox multivariate model (Figs. 4C and 4D). In particular, among patients with negative ^{18}F-FDG PET results ($n = 110$), a high-risk IFM15 signature was still associated with shorter PFS (HR, 3.9 [95% CI, 1.8–8.8] [$P = 0.001$]).

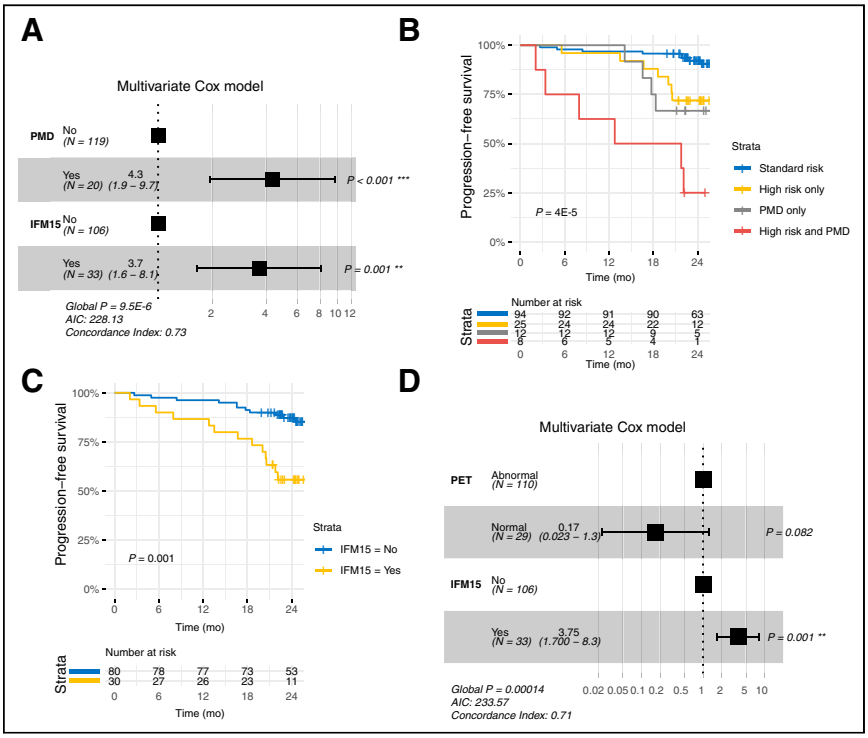

FIGURE 4. Prognostic value of imaging and gene expression profiles. (A) Multivariate Cox modeling of PFS by presence of PMD and high-risk IFM15 gene expression signature (IFM15+). (B) Kaplan–Meier curves representing PFS of MM patients separated by IFM15 and PMD status. (C) Kaplan–Meier curves depicting PFS of patients with positive ^{18}F-FDG PET results only ($n = 110/139$) and according to their IFM15 risk status. (D) Multivariate Cox modeling of PFS using PET (normal or abnormal results) and IFM15 (Yes = high risk; No = standard risk) binary variables. AIC = Akaike information criterion.

DISCUSSION

The last decade witnessed significant progress in the development of risk classifiers derived from cytogenetics and gene expression profiling in newly diagnosed MM (*8,9,15,16*). Yet, intrapatient heterogeneity, inherent to this pathology, might reduce the sensitivity of these tests—which are often based on a single localized sample that does not necessarily reflect the entire pathology (*17*). Thus, whole-body functional imaging such as ^{18}F-FDG PET has been proposed as

a complementary approach for prognosis at baseline. As such, both transcriptomic and imaging approaches allow the identification of patients at high risk of progression, despite the fact that they seem to be opposed in nature. The cells studied in RNA sequencing come from a single, localized bone marrow aspirate, whereas ^{18}F-FDG PET explores whole-body spatial heterogeneity. In this context, some ^{18}F-FDG PET scan results are considered negative or normal despite the clinical diagnosis established, in particular, by the presence of malignant plasma cells in the bone marrow aspirate. Yet, it seems possible that the characteristics of these 2 techniques partially overlap and that the biomarkers described in ^{18}F-FDG PET can find echoes in transcriptomic data beyond the *HK2* underexpression shown by the initial work of Rasche et al. (*3*).

In the present study, we reported novel associations between imaging patterns and gene expression in MM, and we extended our knowledge of the molecular profiles of negative or normal ^{18}F-FDG PET results. Our data demonstrate that normal or negative ^{18}F-FDG PET scan results are associated with the specific expression of glucose metabolism genes and with the LB molecular subgroup, whereas abnormal or positive ^{18}F-FDG PET scan results are associated with markers of cell proliferation and with a distinct transcriptomic profile including the fructose transporter *GLUT5*.

The combination of PMD and the IFM15 signature clearly identified a subset of patients with a higher risk of progression in our cohort. This result was independent of the patients' R-ISS stage and therefore extended the risk classification at diagnosis. The prognostic value of PMD or IFM15 was independent of undetectable MRD or a complete stringent clinical response. Interestingly, the only R-ISS stage 1 patient who was positive for both PMD and IFM15 progressed in 4 mo and died within 2 y. Further studies could extend these observations to overall survival and compare this new biomarker with other very high-risk groups, such as the "Double-Hit" group (*18*).

As for the 7 UAMS molecular subgroups, Usmani et al. previously reported that the PR, MF, and GEP70 subgroups had more EMD (*19*). These observations were not made in the present study, yet the PR and GEP70 subgroups were associated with PMD. To our knowledge, this finding was not reported in previous work. However, the concept of PMD, corresponding to soft-tissue invasion with contiguous bone involvement, is relatively recent. The CASSIOPET prospective study was the first to examine and report the prognostic value of this particular imaging biomarker (*5*). It is plausible that these 2 entities were mixed in previous work, explaining these discordant results.

Patients with negative or normal ^{18}F-FDG PET scan results at diagnosis were more likely to belong to the LB subgroup of the UAMS classification, a consistent result, since this cluster is characterized by a small number of FLs detected on MRI and both groups have a good clinical prognosis. To our knowledge, this observation was not made in previous studies.

We also confirmed the underexpression of *HK2* in this subgroup and showed that *GLUT3* and especially *GLUT5* were deregulated to a greater extent than *HK2* between patients with negative or normal ^{18}F-FDG PET scan results and patients with positive or abnormal ^{18}F-FDG PET scan results. More generally, when we extended our analysis to the genome, 2 gene expression signatures stood out for MM patients with positive ^{18}F-FDG PET results. The first involved proliferation genes (*MKI-67*, *PCNA*, *TOP2A*, *STMN1*) and proliferation groups (PR and MS). The second involved *GLUT5* and lymphocyte antigens (e.g., *CD19*, *CD30 L*, and *TRAIL*), suggesting that a particular gene expression program is associated with glucose avidity independently of proliferation. This observation needs to be validated at the protein level and will be the subject of a prospective study with another cohort.

Similarly, 2 observations that require further investigations were made. First, strong expression of *GLUT5*/*SLC2A5* was associated with positive ^{18}F-FDG PET results. This finding was unexpected, since GLUT5 does not transport glucose but transports fructose (*14(p5)*). High levels of expression of *GLUT5* in ^{18}F-FDG–avid tissues have been reported in the literature as a "discrepancy" in breast cancer cells expressing low levels of *GLUT1* (*20*). Finally, although previously described (*2*), the prognostic value of SUV_{max} using a threshold of 4.2 did not appear to be significant in a multivariate analysis in our work, a result for which bias due to the inherent limitations of SUV calculations in a multicenter study cannot be ruled out.

CONCLUSION

The present study enabled a better characterization of the molecular signature of ^{18}F-FDG PET biomarkers. Moreover, the combined prognostic value of PMD and a high-risk IFM15 signature may help define a group of MM patients with a very high risk of progression. This work demonstrated, once again, the added prognostic value of integrating ^{18}F-FDG PET in the management of MM.

DISCLOSURE

This work was supported by grants from the French National Agency for Research IRON Labex (ANR-11-LABX-0018–01), ArronaxPlusEquipex (ANR-11-EQPX-0004), ISITE NExT (ANR-16-IDEX-0007), SIRIC ILIAD (Imaging and Longitudinal Investigations to Ameliorate Decision-Making in Multiple Myeloma and Breast Cancer), INCA-DGOS-Inserm 12558, and Janssen Research & Development. Philippe Moreau declares being a member of advisory boards for Celgene, Janssen, Takeda, Novartis, and Amgen. Cyrille Touzeau declares fees and consultancy for Celgene, Janssen, Takeda, GlaxoSmithKline, Amgen, Abbvie, and Sanofi. No other potential conflict of interest relevant to this article was reported.

ACKNOWLEDGMENTS

We thank Elise Douillard, Magali Devic, and Nathalie Roi for excellent technical expertise and the Biogenouest sequencing platform GenoBird in Nantes, France, for the Illumina sequencing.

KEY POINTS:

QUESTION: Are baseline ^{18}F-FDG PET biomarkers in newly diagnosed MM patients associated with a specific molecular signature through RNA sequencing?

PERTINENT FINDINGS: Negative results on ^{18}F-FDG PET scans were associated with lower levels of expression of *HK2* and showed enrichment for patients with the LB subgroup, whereas positive results on ^{18}F-FDG PET scans revealed 2 distinct signatures: either high levels of expression of proliferation genes or high levels of expression of *GLUT5* and lymphocyte antigens. The combined prognostic value of PMD and a high-risk IFM15 signature defined a group of MM patients with a very high risk of progression.

IMPLICATIONS FOR PATIENT CARE: A combination of prognostic biomarkers from imaging and gene expression profiling has the potential to improve MM management and may define a novel risk stratification algorithm.

REFERENCES

1. Cavo M, Terpos E, Nanni C, et al. Role of ^{18}F-FDG PET/CT in the diagnosis and management of multiple myeloma and other plasma cell disorders: a consensus statement by the International Myeloma Working Group. *Lancet Oncol.* 2017;18: e206–e217.
2. Michaud-Robert A-V, Jamet B, Bailly C, et al. FDG-PET/CT, a promising exam for detecting high-risk myeloma patients? *Cancers (Basel).* 2020;12:1384.
3. Rasche L, Angtuaco E, McDonald JE, et al. Low expression of hexokinase-2 is associated with false-negative FDG–positron emission tomography in multiple myeloma. *Blood.* 2017;130:30–34.
4. Abe Y, Ikeda S, Kitadate A, et al. Low hexokinase-2 expression-associated false-negative ^{18}F-FDG PET/CT as a potential prognostic predictor in patients with multiple myeloma. *Eur J Nucl Med Mol Imaging.* 2019;46:1345–1350.
5. Moreau P, Zweegman S, Perrot A, et al. Evaluation of the prognostic value of positron emission tomography-computed tomography (PET-CT) at diagnosis and follow-up in transplant-eligible newly diagnosed multiple myeloma (TE NDMM) patients treated in the phase 3 Cassiopeia study: results of the Cassiopet companion study. *Blood.* 2019;134(suppl 1):692.
6. Zhan F, Huang Y, Colla S, et al. The molecular classification of multiple myeloma. *Blood.* 2006;108:2020–2028.
7. Broyl A, Hose D, Lokhorst H, et al. Gene expression profiling for molecular classification of multiple myeloma in newly diagnosed patients. *Blood.* 2010;116:2543–2553.
8. Shaughnessy JD, Zhan F, Burington BE, et al. A validated gene expression model of high-risk multiple myeloma is defined by deregulated expression of genes mapping to chromosome 1. *Blood.* 2007;109:2276–2284.
9. Decaux O, Lodé L, Magrangeas F, et al. Prediction of survival in multiple myeloma based on gene expression profiles reveals cell cycle and chromosomal instability signatures in high-risk patients and hyperdiploid signatures in low-risk patients: a study of the Intergroupe Francophone du Myélome. *J Clin Oncol.* 2008; 26:4798–4805.
10. Moreau P, Attal M, Hulin C, et al. Bortezomib, thalidomide, and dexamethasone with or without daratumumab before and after autologous stem-cell transplantation for newly diagnosed multiple myeloma (CASSIOPEIA): a randomised, open-label, phase 3 study. *Lancet.* 2019;394:29–38.
11. Barwick BG, Neri P, Bahlis NJ, et al. Multiple myeloma immunoglobulin lambda translocations portend poor prognosis. *Nat Commun.* 2019;10:1911.
12. Michaud-Robert A-V, Zamagni E, Carlier T, et al. Glucose metabolism quantified by SUVmax on baseline FDG-PET/CT predicts survival in newly diagnosed multiple myeloma patients: combined harmonized analysis of two prospective phase III trials. *Cancers (Basel).* 2020;12:2532.
13. Kumar S, Paiva B, Anderson KC, et al. International Myeloma Working Group consensus criteria for response and minimal residual disease assessment in multiple myeloma. *Lancet Oncol.* 2016;17:e328–e346.
14. Nomura N, Verdon G, Kang HJ, et al. Structure and mechanism of the mammalian fructose transporter GLUT5. *Nature.* 2015;526:397–401.
15. Avet-Loiseau H, Li C, Magrangeas F, et al. Prognostic significance of copy-number alterations in multiple myeloma. *J Clin Oncol.* 2009;27:4585–4590.
16. Avet-Loiseau H, Attal M, Moreau P, et al. Genetic abnormalities and survival in multiple myeloma: the experience of the Intergroupe Francophone du Myélome. *Blood.* 2007;109:3489–3495.
17. Rasche L, Chavan SS, Stephens OW, et al. Spatial genomic heterogeneity in multiple myeloma revealed by multi-region sequencing. *Nat Commun.* 2017;8:268.
18. Walker BA, Mavrommatis K, Wardell CP, et al. A high-risk, Double-Hit, group of newly diagnosed myeloma identified by genomic analysis. *Leukemia.* 2019;33: 159–170.
19. Usmani SZ, Heuck C, Mitchell A, et al. Extramedullary disease portends poor prognosis in multiple myeloma and is over-represented in high-risk disease even in the era of novel agents. *Haematologica.* 2012;97:1761–1767.
20. Hamann I, Krys D, Glubrecht D, et al. Expression and function of hexose transporters GLUT1, GLUT2, and GLUT5 in breast cancer: effects of hypoxia. *FASEB J.* 2018;32:5104–5118.